ACS Chemical Neuroscience

Research Article

pubs.acs.org/chemneuro

Anti-Inflammatory Activity of Iridoid and Catechol Derivatives from *Eucommia ulmoides* Oliver

Dan Luo,[†] Terry C. T. Or,[†] Cindy L. H. Yang,*[,†] and Allan S. Y. Lau*[,†,‡]

[†]Molecular Chinese Medicine Laboratory, Li Ka Shing Faculty of Medicine, The University of Hong Kong, Hong Kong Special Administrative Region, China

[‡]Cytokine Biology Group, Department of Paediatrics and Adolescent Medicine, The University of Hong Kong, Hong Kong Special Administrative Region, China

Supporting Information

ABSTRACT: Neuroinflammation and pro-inflammatory mediators play key roles in the pathogenesis of neurodegenerative diseases including stroke, which account for a significant burden of morbidity and mortality worldwide. Recently, the unsatisfactory pharmacotherapy and side effects of the drugs led to the development of alternative medicine for treating these diseases. Du Zhong (DZ), *Eucommia ulmoides* Oliver leaves, is a commonly used herb in the therapy of stroke in China. We hypothesize that the components from DZ inhibit neuroinflammation. In this study, DZ was extracted and the bioactive fractions with inhibitory effect on lipopolysaccharide (LPS)-stimulated nitric oxide (NO) production in BV-2 microglial cells were further separated using chromatography. Two purified bioactive compounds, genipin (compound C) and 4-(1,2-dimethoxyethyl)benzene-1,2-diol (compound F), were isolated and identified after spectroscopic analysis. The results showed that they inhibited LPS-stimulated NO and tumor necrosis factor-alpha (TNF-α) production. Genipin exerted its anti-inflammatory effects through PI3K/Akt signaling pathway, whereas compound F inhibited phosphorylation of p38 mitogen-activated protein kinase (MAPK). In conclusion, genipin and compound F have potential for developing into new drugs for treating neurodegenerative diseases.

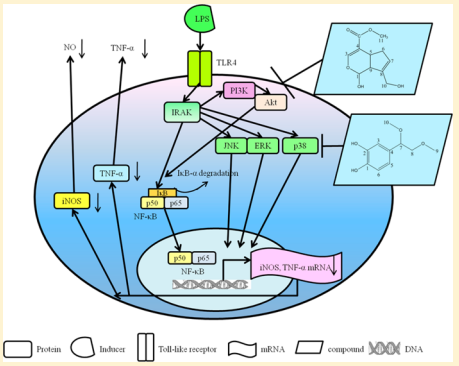

KEYWORDS: *Neuroinflammation, Eucommia ulmoides Oliver, neurodegenerative diseases, genipin, 4-(1,2-dimethoxyethyl)benzene-1,2-diol*

Neuroinflammation has been considered as one of the pathological factors in neurodegenerative diseases including Alzheimer's disease (AD), Parkinson's disease (PD), stroke, dementia, and amyotrophic lateral sclerosis (ALS).[1] It refers to the reaction of the endogenous central nervous system (CNS) in response to various pathological stimuli including endotoxins and neurotoxins.[2] Microglia, the brain resident macrophages, are first activated to represent the first line of defense in the CNS, in which they are morphologically transformed into phagocytes and phagocytose the infectious microbes and dead or dying cells in the CNS.[3] However, overactivation of microglia leads to the secretion of various proinflammatory mediators including tumor necrosis factor-alpha (TNF-α), interleukin-1 beta (IL-1β), interleukin-6 (IL-6), nitric oxide (NO), and reactive oxygen species (ROS), resulting in neuronal cell death.[4,5] Therefore, inhibition of microglia activation and subsequent neuroinflammation may be a potential therapeutic target for neurodegenerative diseases.

NO is regarded as one of the main pathological mediators in neuroinflammation.[6] It is synthesized from L-arginine by the enzyme nitric oxide synthase (NOS)[7] isoforms including neuronal NOS (nNOS), endothelial NOS (eNOS), and inducible NOS (iNOS). iNOS is the most relevant to neuroinflammation, and it generates a micromolar amount of NO when induced.[8] In addition, NO and superoxide lead to the formation of peroxynitrite, which results in numerous oxidation and potential destruction of host cellular constituents causing dysfunctional critical cellular processes, cell signaling pathway disruption, and brain cell death via cell apoptosis and necrosis.[9,10]

TNF-α is another proinflammatory mediator known to be implicated in neurodegenerative diseases.[11] Upon CNS damage/infection, elevated levels of TNF-α had been shown to be synthesized by astrocytes, neurons, and microglia.[12] The resulting TNF-α can induce IL-1 and IL-6 production, which aggravates neuroinflammatory related neurodegenerative diseases.[13] By inhibiting TNF-α production, the brain injury in mice model was reduced and intercellular adhesion molecule-1 expression was attenuated during transient cerebral ischemia.[14]

Microglial activation triggers the production of inflammatory mediators through various signaling pathways including mitogen-activated protein kinase (MAPKs: c-Jun N-terminal kinase (JNK), p38 kinase, and extracellular signal-regulated kinase (ERK)) and PI3K/Akt. They transduce the extracellular

Received: December 6, 2013
Revised: July 16, 2014
Published: July 26, 2014

ACS Publications © 2014 American Chemical Society

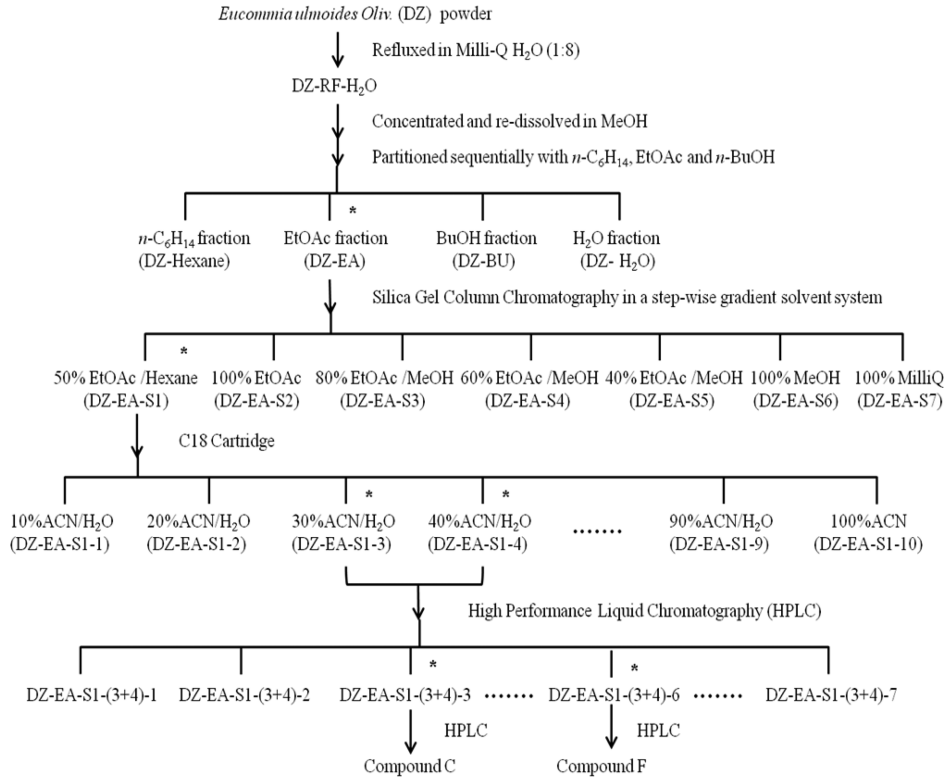

Figure 1. Extraction and separation scheme of compounds C and F from *Eucommia ulmoides* Oliver (DZ). An amount of 15 g of DZ powder was macerated in Milli-Q water for 2 h and then refluxed for another 2.5 h. After drying, the aqueous extract was dissolved in 100 mL of methanol (MeOH) and then partitioned sequentially with 100 mL of hexane (n-C_6H_{14}), 100 mL of ethyl acetate (EtOAc), and 100 mL of butanol (n-BuOH). The fractions with the most potent inhibition on LPS-stimulated NO production were selected and then subjected to silica gel chromatography and C18 solid phase extraction, and further purified by reversed-phase high-performance liquid chromatography (HPLC) using gradient elution until two single compounds (compound C and F) with anti-inflammatory effects were obtained. *Fractions showed potent NO inhibition in LPS-induced BV-2 cells.

stimuli through a cascade of protein phosphorylations, which leads to the activation of transcription factor nuclear factor (NF)-κB.[15] Previous studies indicated that p38 kinase, ERK, and JNK were phosphorylated in the LPS/IFN-γ activated mice or human microglia.[16−18] By suppressing p38 kinase as well as ERK signaling pathways, the areas of brain injury were reduced in ischemia−reperfusion mouse/rat models.[19,20] The PI3K/Akt pathway was activated by LPS-stimulated peripheral blood mononuclear cells (PBMCs), whereas inhibition of the PI3K/Akt pathway resulted in significant reduction of inflammatory cytokines.[21] NF-κB is a transcription factor, and it is believed to play an essential role in activating inflammatory related genes in response to immunostimulation.[22] Upon stimulation, the NF-κB p65 subunit is activated, leading to IκB degradation and NF-κB nuclear translocation, which is responsible for the transcriptional activation of the inflammation-related genes including TNF-α and iNOS.[23,24] Therefore, transcriptional regulation can be the important therapeutic target for neuroinflammation therapy.

Du Zhong (DZ), *Eucommia ulmoides* Oliver leaves, is a commonly used herb for the treatment of stroke and hypertension related symptoms including hemiplegia, dizziness, vertigo, and neurasthenia in China. These symptoms also can be observed in patients with AD and PD.[25] Studies demonstrated the effect of DZ on decreasing blood pressure in spontaneous hypertensive rats.[26,27] Besides, it also showed antiobesity and antioxidative effects in mice models.[28,29] Previous studies of DZ were mainly focused on the vascular-related hypertension and diabetes related diseases, whereas its effect on neuroinflammation is largely unknown.

Here, we determine the anti-inflammatory effect of the herb DZ on LPS-activated microglial cells. We use a bioactivity-guided fractionation scheme involving the sequential use of partitioning extraction and high performance liquid chromatography (HPLC) to isolate and identify the potent compounds that can inhibit NO production from DZ. The purified compounds were analyzed by using gas chromatographymass spectrometry (GC/MS) and nuclear magnetic resonance (NMR). We further delineated the underlying mechanisms of the anti-inflammatory effect of the identified compounds. Our findings may be useful for the development of adjunctive therapeutic agents for treating neurodegenerative diseases.

RESULTS AND DISCUSSION

Isolation and Identification of Anti-Inflammatory Compounds from DZ. Neurodegenerative diseases, sharing the same pathological mechanism of neuroinflammation, account for an increase of morbidity and mortality in patients, and the population is estimated to be over 60 million by 2050.[30] Recently, the unsatisfactory pharmacotherapy and side effects of the drugs led to the development of alternative medicine for treating these diseases.[31]

DZ leaf contains different groups of compounds including polyphenolics (pyrogallol, protocatechuic acid, coumaric acid, and chlorogenic acid), flavonoids (quercetin, kaempherol, and astragarin), and triterpines.[32] In this study, we aimed to isolate

dx.doi.org/10.1021/cn5001205 | ACS Chem. Neurosci. 2014, 5, 855−866

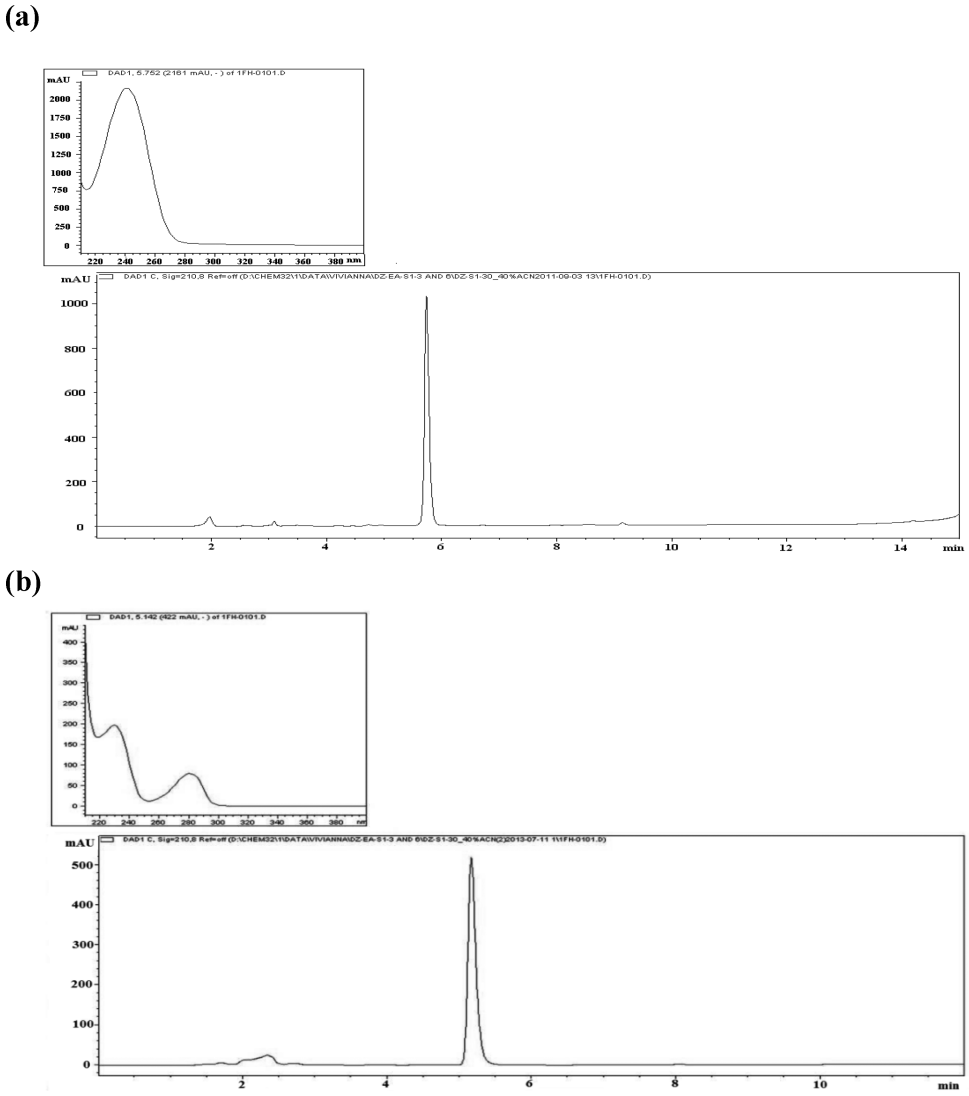

Figure 2. (a) HPLC chromatogram and UV absorbance spectrum of compound C. Compound C was purified using HPLC (Eclipse XDB-C18, 5 μm 4.6 × 250 mm, Agilent) at a flow rate of 1 mL/min with a gradient elution from 20% to 90% ACN. The detection wavelength was set at 210 nm. The compound was eluted at approximately 5.75 min with UV absorbance maximized at 240 nm. (b) HPLC chromatogram and UV absorbance spectrum of compound F. Compound F was purified using HPLC (Eclipse XDB-C18, 5 μm 4.6 × 250 mm, Agilent) at a flow rate of 1 mL/min with a gradient elution from 40% to 50% ACN. The detection wavelength was set at 210 nm. The compound was eluted at approximately 5.16 min with UV absorbance maximized at 230 and 280 nm.

compounds that inhibited NO production in LPS-stimulated BV-2 cells. The extraction scheme is summarized in Figure 1. The chemicals in the aqueous extract of DZ (DZ-RF-H_2O) were separated by solvent partition. As only small amount of *n*-C_6H_{14} fraction (DZ-Hexane) was obtained, we focused on the EtOAc fraction (DZ-EA), BuOH fraction (DZ-BU), and aqueous fraction (DZ-H_2O). Among the fractions, DZ-EA at the concentration up to 50 μg/mL did not show cytotoxicity to BV-2 cells and it showed the potent inhibitory effect on NO production in LPS-stimulated BV-2 cells ($p < 0.05$) (Supporting Information Figure S1). After silica gel column chromatography, DZ-EA was separated into seven fractions. The result showed that DZ-EA-S1 had the strongest suppressive effect among the fractions ($p < 0.01$) (Figure S2). Using C18 solid phase extraction, DZ-EA-S1-3 and DZ-EA-S1-4 without showing cytotoxicity were obtained, and they significantly inhibited NO production ($p < 0.01$) (Figure S3). Thus, they were combined as DZ-EA-S1-(3 + 4) and then further separated by HPLC. The results showed that the nontoxic fractions including DZ-EA-S1-(3 + 4)-3 and DZ-EA-S1-(3 + 4)-6 had the most potent inhibitory effect on LPS-stimulated NO production (data not shown). After purification, one single compound (compound C) with 95% chemical purity was eluted at approximately 5.75 min with UV absorbance maximized at 240 nm (Figure 2a). Another single compound (compound F) was eluted at approximately 5.16 min with UV absorbance maximized at 230 and 280 nm (Figure 2b).

Compound C is white crystals with UV absorbance maximized at 240 nm, which is a characteristic of an iridoid compound. The ^{13}C NMR and ^{1}H NMR spectra of compound C are shown in Figure S4. The ^{13}C NMR (CD_3OD) spectrum showed signals at δ170.0 ($-CO_2-$), 97.8 (C-1), 154.4 (C-3), 111.8 (C-4), 51.8 (C-5), 40.1 (C-6), 128.3 (C-7), 145.7 (C-8), 48.5 (C-9), 61.8 (C-10), and 37.7 (C-11). The carbon signals indicated that the compound contained two cyclic ethylene groups (C-3 and C-4) and (C-7 and C-8), one carbonyl group

dx.doi.org/10.1021/cn5001205 | *ACS Chem. Neurosci.* 2014, 5, 855−866

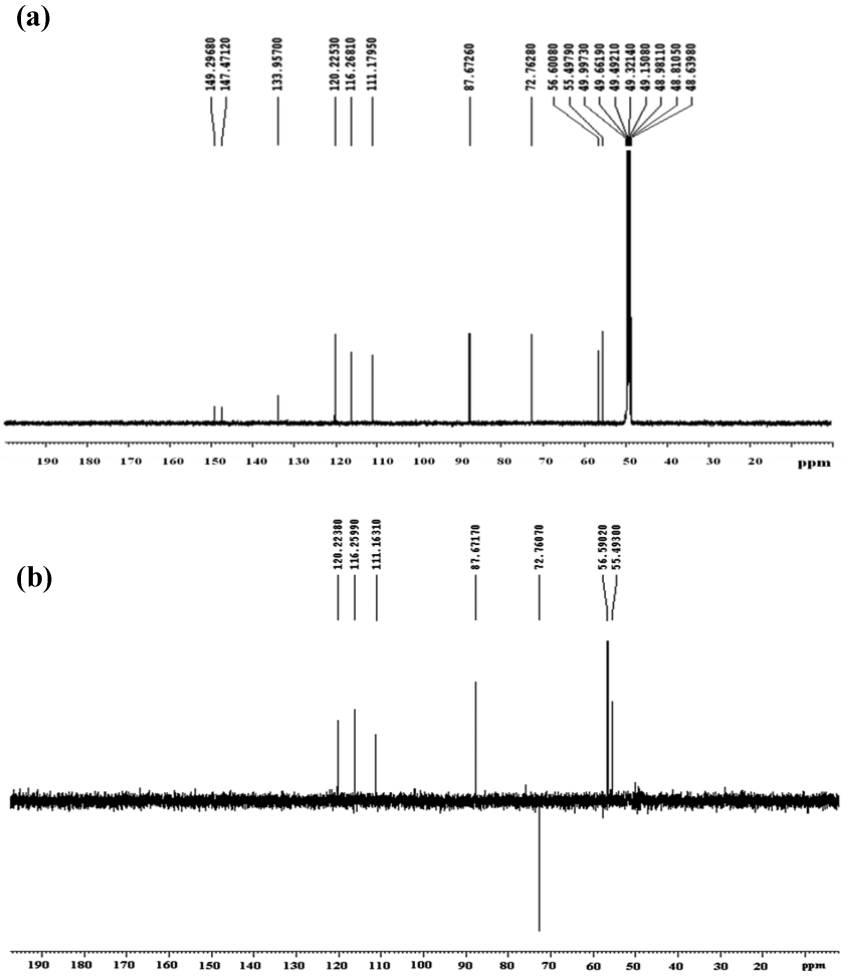

Figure 3. (a) ^{13}C NMR and (b) Dept 135 NMR spectra of compound F. The structure of compound F was elucidated using a Bruker 600-MH_Z PRX NMR spectrometer. Methanol-*d* was used as the solvent. The ^{13}C NMR spectrum showed signals at δ 149.3 (C-1), 147.5 (C-2), 120.2 (C-3), 134.0 (C-4), 111.2 (C-5), 116.3 (C-6), 87.7 (C-7), 72.7 (C-8), 56.6 (C-9), and 55.5 (C-10). From Dept 135, compound F contains two methyls (C-9, C-10), one methylene (C-8), three methines (C-3, C-5, C-6), three quaternary carbons (C-1, C-2, C-4), and one secondary carbon (C-7). Therefore, compound F is identified as 4-(1,2-dimethoxyethyl)benzene-1,2-diol.

($-CO_2-$), one methoxy group (C-11), and three methine groups (C-1, 5, 9). Electron ionization mass spectra showed that compound C had a mass to charge ratio at $[M]^+$ 226, 208, 190, 176, 148, 120, 91, 78, 67, and 51. The ion at 226 corresponds to the molecular formula $C_{11}H_{14}O_5$. In comparison to the spectroscopic data with the data reported in the literature, compound C was identified as genipin and its molecular weight is 226.1 (Figure 4a).[33,34] Genipin is a well characterized constituent of *Eucommia* plants whose biological activities have been well characterized. Compound F is yellow crystals. The ^{13}C NMR spectra of compound F (Figure 3a) showed signals at δ 149.3 (C-1), 147.5 (C-2), 120.2 (C-3), 134.0 (C-4), 111.2 (C-5), 116.3 (C-6), 87.7 (C-7), 72.7 (C-8), 56.6 (C-9), and 55.5 (C-10). From Dept 135 experiment (Figure 3b), compound F contained two methyls (C-9, C-10), one methylene (C-8), three methines (C-3, C-5, C-6), three quaternary carbons (C-1, C-2, C-4), and one secondary carbon (C-7). Therefore, compound F was identified as 4-(1,2-dimethoxyethyl)benzene-1,2-diol, and its molecular weight is 198.1 (Figure 4b).

The Effects of Genipin and Compound F on NO, mRNA, and Protein Levels of iNOS and TNF-α in LPS-Stimulated BV-2 Cells. We examined the effect of genipin

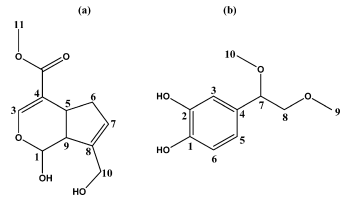

Figure 4. Chemical structures of (a) genipin (compound C) and (b) 4-(1,2-dimethoxyethyl)benzene-1,2-diol (compound F).

and compound F on LPS-stimulated NO production in BV-2 microglial cells. Our results showed that BV-2 cells stimulated with LPS (100 ng/mL) markedly increased NO production when compared with the control group not treated with LPS. With the pretreatment of genipin or compound F, NO production was inhibited in a dose-dependent manner (Figure 5). The NO production was significantly reduced by 90% and 45% after treating the cells with 25 μg/mL genipin and 50 μg/mL compound F, respectively ($p < 0.01$). To exclude the possibility that the reduction of NO production was attributed to the cytotoxicity of genipin and compound F, BV-2 cell viability was evaluated using MTT assays. Cells were treated with genipin or compound F at indicated concentrations (5, 10,

dx.doi.org/10.1021/cn5001205 | ACS Chem. Neurosci. 2014, 5, 855−866

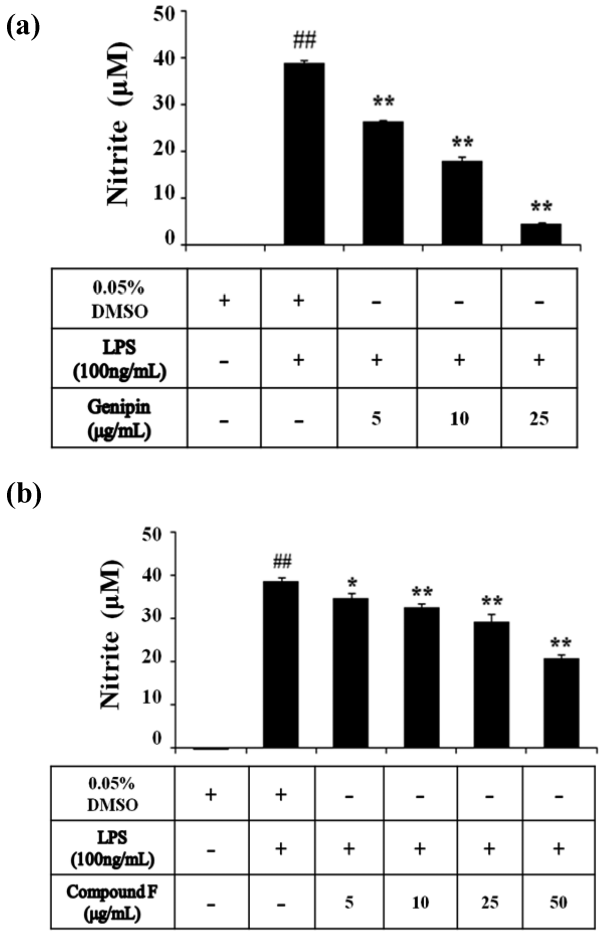

Figure 5. (a) Effect of genipin on NO production in LPS-stimulated BV-2 cells. BV-2 cells were pretreated with 0.025% DMSO or genipin (5, 10, and 25 μg/mL) for 2 h, followed by the stimulation of LPS (100 ng/mL) for another 24 h. The supernatants were collected for the nitrite measurement using Griess reagent. All data are presented as mean ± SD of three independent experiments. $^{\#\#}p < 0.01$, compared with DMSO group. $^{*}p < 0.05$, $^{**}p < 0.01$, compared with DMSO + LPS group. (b) Effect of compound F on NO production in LPS-stimulated BV-2 cells. BV-2 cells were pretreated with 0.025% DMSO or compound F (5, 10, 25, and 50 μg/mL) for 2 h, followed by the stimulation of LPS (100 ng/mL) for another 24 h. The supernatants were collected for the nitrite measurement using Griess reagent. All data are presented as mean ± SD of three independent experiments. $^{\#\#}p < 0.01$, compared with DMSO group. $^{*}p < 0.05$, $^{**}p < 0.01$, compared with DMSO + LPS group.

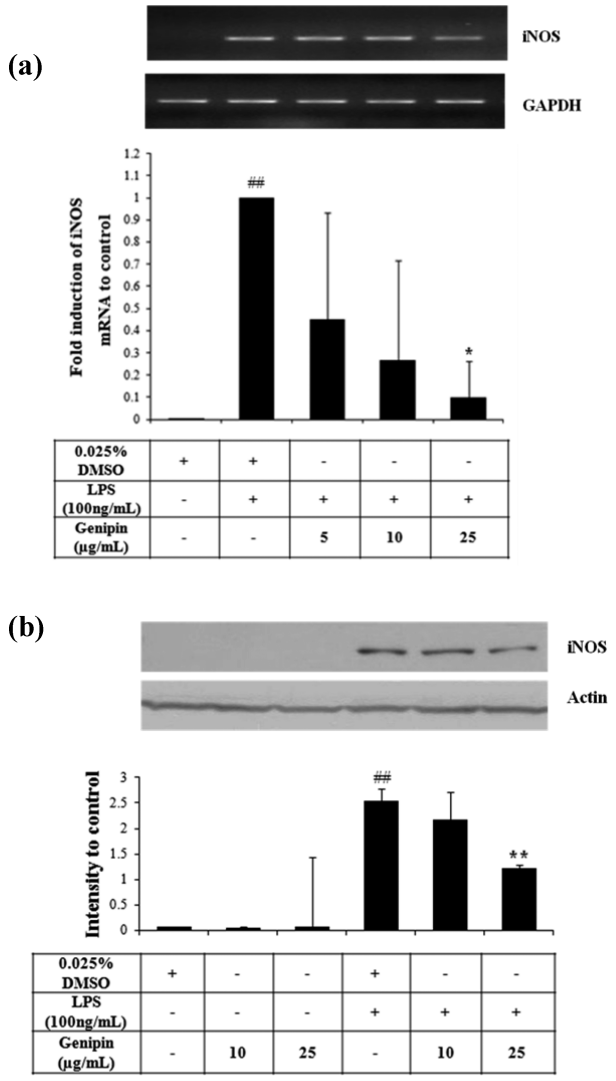

Figure 6. (a) Effect of genipin on iNOS mRNA level in LPS-stimulated BV-2 cells. BV-2 cells were pretreated with genipin (5, 10, and 25 μg/mL) for 2 h, followed by the stimulation of LPS (100 ng/mL) for another 3 h. Total RNA was then extracted and subjected to quantitative-PCR. The mRNA levels were normalized with actin. All data are presented as mean ± SD of three independent experiments. $^{\#\#}p < 0.01$, compared with DMSO group. $^{*}p < 0.05$, compared with DMSO + LPS group. (b) Effect of genipin on iNOS protein expression in LPS-stimulated BV-2 cells. BV-2 cells were pretreated with genipin (10 and 25 μg/mL) for 2 h, followed by the stimulation of LPS (100 ng/mL) for another 24 h. The protein expression of iNOS was then determined by Western blot. Actin was used to confirm equal loading of samples. The figures shown are representative of three independent experiments. $^{\#\#}p < 0.01$, compared with DMSO group. $^{**}p < 0.01$, compared with DMSO + LPS group.

25, and 50 μg/mL) for 48 h. It was found that genipin and compound F did not affect BV-2 cell viability (data not shown), which revealed that they were not toxic to microglial cells up to the concentration of 50 μg/mL.

From the above results, genipin and compound F showed potent inhibition on LPS-stimulated NO production in BV-2 microglial cells. We then investigated whether they could inhibit mRNA levels of LPS-stimulated iNOS at the transcriptional level. Cells were pretreated with genipin or compound F for 2 h prior to 100 ng/mL LPS stimulation for 3 h. The result showed that LPS induced the mRNA level of iNOS in BV-2 cells. With the pretreatment of genipin or compound F, the mRNA level of iNOS was reduced in a dose-dependent manner (Figures 6a and 7a). Moreover, Quantitative RT-PCR was performed to confirm their inhibitory effects. When compared with the control (DMSO + LPS) group, genipin at a concentration of 25 μg/mL and compound F at a concentration of 50 μg/mL inhibited 90% and 68% of mRNA level of iNOS, respectively ($p < 0.05$) (Figures 6a and 7a). In addition, it was also found that the protein expression of iNOS was significantly reduced after the pretreatment of 25 μg/mL genipin or 50 μg/mL compound F in LPS-stimulated BV-2 cells ($p < 0.01$) (Figures 6b and 7b). The results revealed that genipin and compound F both possessed an anti-inflammatory effect by suppressing the gene and protein expressions of iNOS.

dx.doi.org/10.1021/cn5001205 | ACS Chem. Neurosci. 2014, 5, 855−866

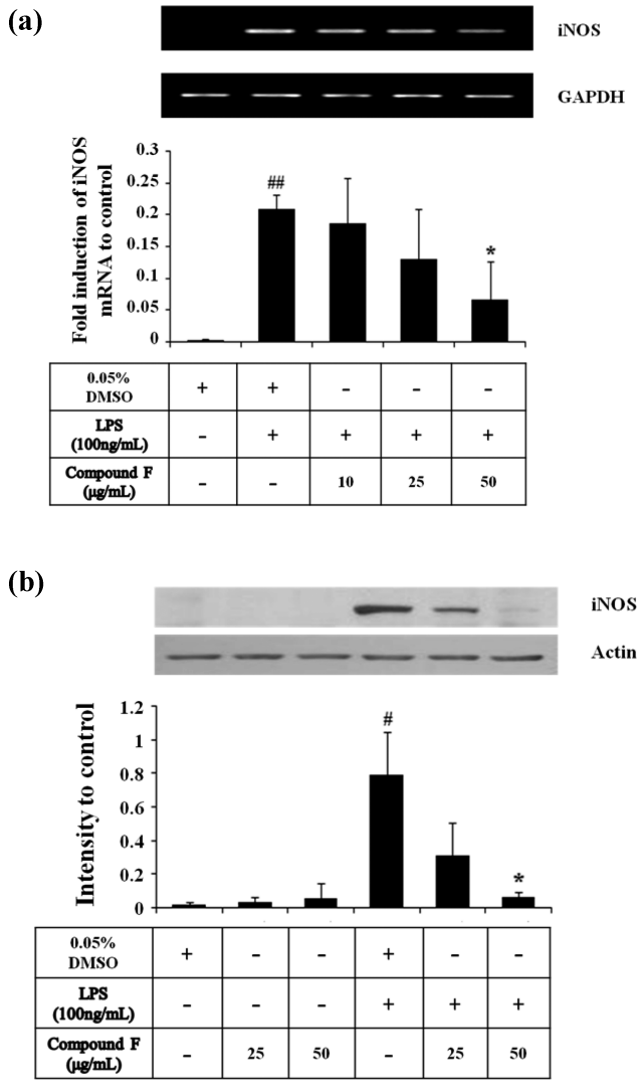

Figure 7. (a) Effect of compound F on iNOS mRNA level in LPS-stimulated BV-2 cells. BV-2 cells were pretreated with compound F (10, 25, and 50 μg/mL) for 2 h, followed by the stimulation of LPS (100 ng/mL) for another 3 h. Total RNA was then extracted and subjected to quantitative-PCR. The mRNA levels were normalized with actin. All data are presented as mean ± SD of three independent experiments. $^{\#\#}p < 0.01$, compared with DMSO group. $^{*}p < 0.05$, compared with DMSO + LPS group. (b) Effect of compound F on iNOS protein expression in LPS-stimulated BV-2 cells. BV-2 cells were pretreated with compound F (25 and 50 μg/mL) for 2 h, followed by the stimulation of LPS (100 ng/mL) for another 24 h. The protein expression of iNOS was then determined by Western blot. Actin was used to confirm the equal loading of samples. The figures shown are representative of three independent experiments. $^{\#}p < 0.05$, compared with DMSO group. $^{*}p < 0.05$, compared with DMSO + LPS group.

To investigate whether genipin and compound F can inhibit mRNA level of LPS-stimulated TNF-α, we pretreated BV-2 cells with genipin or compound F for 2 h prior to the stimulation of 100 ng/mL LPS for another 3 h. The result showed that the mRNA level of TNF-α was increased in LPS-stimulated BV-2 cells. With the pretreatment of genipin or compound F, the mRNA level of TNF-α was dose-dependently reduced as measured by both semiquantitative and quantitative RT-PCR (Figures 8 and 9). Moreover, genipin (25 μg/mL) and compound F (50 μg/mL) suppressed 35% and 64.7% of mRNA level of TNF-α when compared with the control

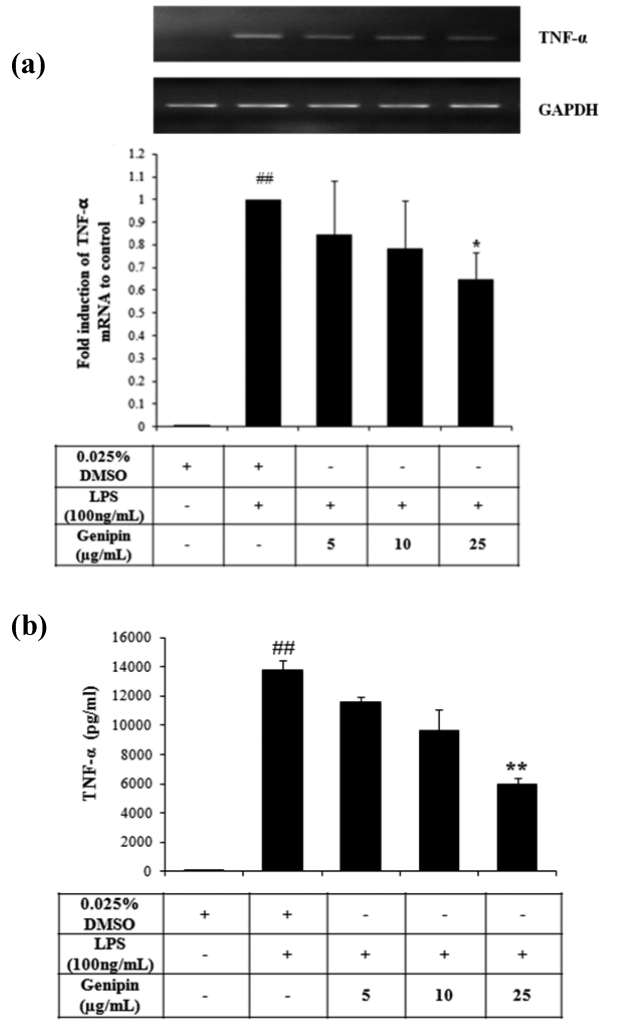

Figure 8. (a) Effect of genipin on TNF-α mRNA level in LPS-stimulated BV-2 cells. BV-2 cells were pretreated with genipin (5, 10, and 25 μg/mL) for 2 h, followed by the stimulation of LPS (100 ng/mL) for another 3 h. Total RNA was then extracted and subjected to quantitative-PCR. The mRNA levels were normalized with actin. All data are presented as mean ± SD of three independent experiments. $^{\#\#}p < 0.01$, compared with DMSO group. $^{*}p < 0.05$, compared with DMSO + LPS group. (b) Effect of genipin on TNF-α production in LPS-stimulated BV-2 cells. BV-2 cells were pretreated with genipin (5, 10, and 25 μg/mL) for 2 h, followed by the stimulation of LPS (100 ng/mL) for another 24 h. TNF-α production was then determined by ELISA. All data are presented as mean ± SD of three independent experiments. $^{\#\#}p < 0.01$, compared with DMSO group. $^{**}p < 0.01$, compared with DMSO + LPS group.

(DMSO+LPS) group, respectively ($p < 0.05$) (Figures 8a and 9a). Moreover, the results were confirmed by ELISA that genipin and compound F suppressed the production of TNF-α by 57% and 60.1%, respectively ($p < 0.01$) (Figures 8b and 9b).

Genipin is a natural iridoid compound and the aglycone of geniposide. Various studies demonstrated that genipin possessed pharmacological effects including anticancer,[35] antithrombosis,[36] neuroprotective,[37] choleretic,[38] antiviral effects,[39] antiangiogenic, and anti-inflammatory agents.[40] Studies showed that genipin could inhibit TNF-α-stimulated expression of vascular cell adhesion molecule-1 (VCAM-1) in human umbilical vein endothelial cells (HUVEC) for treating cardiovascular diseases.[41] Besides, it inhibited nitric oxide production in activated RAW 264.7 murine macrophage cells

dx.doi.org/10.1021/cn5001205 | ACS Chem. Neurosci. 2014, 5, 855−866

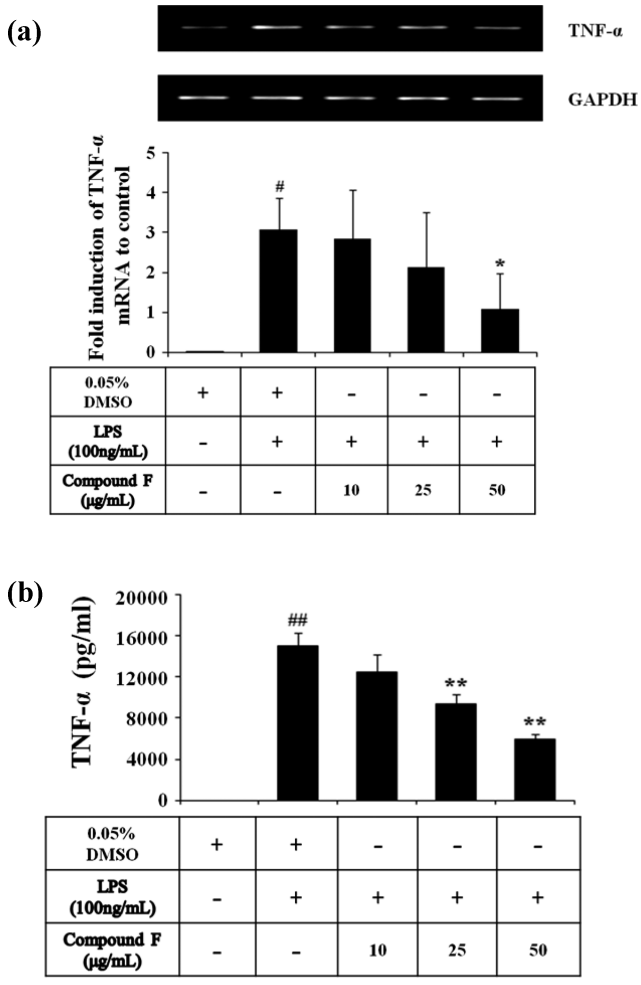

Figure 9. (a) Effect of compound F on TNF-α mRNA level in LPS-stimulated BV-2 cells. BV-2 cells were pretreated with compound F (10, 25, and 50 μg/mL) for 2 h, followed by the stimulation of LPS (100 ng/mL) for another 3 h. Total RNA was then extracted and subjected to quantitative-PCR. The mRNA levels were normalized with actin. All data are presented as mean ± SD of three independent experiments. $^{\#}p < 0.05$, compared with DMSO group. $^{*}p < 0.05$, compared with DMSO + LPS group. (b) Effect of compound F on TNF-α production in LPS-stimulated BV-2 cells. BV-2 cells were pretreated with compound F (10, 25, and 50 μg/mL) for 2 h, followed by the stimulation of LPS (100 ng/mL) for another 24 h. TNF-α production was then determined by ELISA. All data are presented as mean ± SD of three independent experiments. $^{\#\#}p < 0.01$, compared with DMSO group. $^{**}p < 0.01$, compared with DMSO + LPS group.

and LPS-stimulated rat microglia.[42] It also decreased LPS-stimulated TNF-α, IL-1β, prostaglandin E2, and intracellular reactive oxygen species production.[42] Our results showed that genipin inhibited nitric oxide, mRNA, and protein levels of iNOS (Figures 5a and 6) as well as TNF-α production in LPS-stimulated BV-2 cells (Figure 8b), which is in agreement with the previous study.[42]

4-(1,2-Dimethoxyethyl)benzene-1,2-diol (compound F), a novel structure of catechol derivative, was also isolated from DZ extract. Previous studies found that the catechol and its derivatives showed potent anti-inflammatory effects by inhibiting LPS-induced NO and TNF-α production as well as the mRNA and protein levels of iNOS and TNF-α in BV-2 cells.[43] Norepinephrine (NE) and epinephrine (EPI) are well-known catechol derivatives, which show strong anti-inflammatory effects.[44] NE suppressed Aβ-induced mouse microglial cytokine and chemokine production as well as proinflammatory genes at the transcriptional level when it released diffusely in the brain from locus ceruleus (LC).[44] At the same time, it increased microglial migration and phagocytosis of Aβ. In vivo studies also reported that NE deficiency triggered neuroinflammatory conditions and reduced Aβ clearance in animal models of AD.[45] Besides, NE suppressed the enhanced mRNA and protein levels of TNF-α in the LPS-induced primary cultured microglia.[46] EPI was reported to inhibit the production of superoxide in *N*-formyl-methionyl-leucyl-phenylalanine (FMLP) activated human neutrophils.[47] It is also demonstrated to reduce proinflammatory cytokines as measured by decreased TNF-α, IL-6, and IL-8 production in response to LPS induction in blood plasma of healthy volunteers.[48] In this study, we found that compound F (Figure 4b), with similar structure to NE and EPI dose-dependently inhibited LPS-induced iNOS protein expression and mRNA levels of iNOS and TNF-α in BV-2 microglial cells (Figures 7 and 9). Therefore, compound F may have potential to be used as an anti-neuroinflammatory agent.

The Underlying Mechanisms of the Anti-Inflammatory Effect of Genipin and Compound F. To investigate the underlying mechanisms of the anti-inflammatory effect of genipin and compound F, we examined their effects on the phosphorylation of LPS-stimulated MAPKs (p38 kinase, JNK, and ERK). Cells were pretreated with genipin or compound F for 2 h prior to the addition of LPS for 30 min. The results showed that genipin did not affect the activation of MAPKs (Figure10a), whereas compound F at 50 μg/mL significantly suppressed LPS-stimulated phosphorylation of p38 kinase when compared with the control (DMSO + LPS) group ($p < 0.05$) (Figure 10b). However, compound F did not exert any inhibitory effect on LPS-stimulated JNK and ERK activation (Figure 10b). These results indicated that the suppressive effect of genipin on iNOS and TNF-α production was not via MAPK activation, whereas compound F was through p38 kinase signaling pathway. In addition, the effect of genipin and compound F on NF-κB p65 nuclear translocation was further investigated. Our results revealed that the inhibitory effects of genipin (Figure S5) and compound F (Figure 12) were both independent of NF-κB signaling pathway. NF-κB and MAPKs pathways have been regarded as the key targets for inflammatory diseases, as they regulate proinflammatory gene expressions.[49] p38 kinase has been implicated in the signal transduction pathways by increasing iNOS and TNF-α gene expression in glial cells or macrophages.[50] From our study, the effect of compound F on LPS-stimulated translocation of NF-κB p65 of BV-2 cells is examined. The results indicated that compound F did not affect the translocation of NF-κB p65 into the nucleus (Figure 12). Previous studies have also investigated the underlying mechanisms of anti-inflammatory effect of catechol derivatives.[43] Catechol and its derivatives including 3-methylcatechol, 4-methylcatechol, and 4-*tert*-butylcatechol were demonstrated to inhibit the phosphorylation of p38 kinase, nuclear translocation of NF-κB p65, and degradation of IκB in BV-2 cells.[43] Therefore, the results revealed that catechol derivatives including compound F inhibited iNOS and TNF-α gene expression in microglia through p38 kinase signaling pathway.

Besides MAPKs, the PI3K/Akt signaling pathway is also involved in the microglial activation. The effect of genipin on LPS-stimulated phosphorylation of PI3K/Akt was then determined. As shown in Figure 11, genipin suppressed LPS-

dx.doi.org/10.1021/cn5001205 | ACS Chem. Neurosci. 2014, 5, 855−866

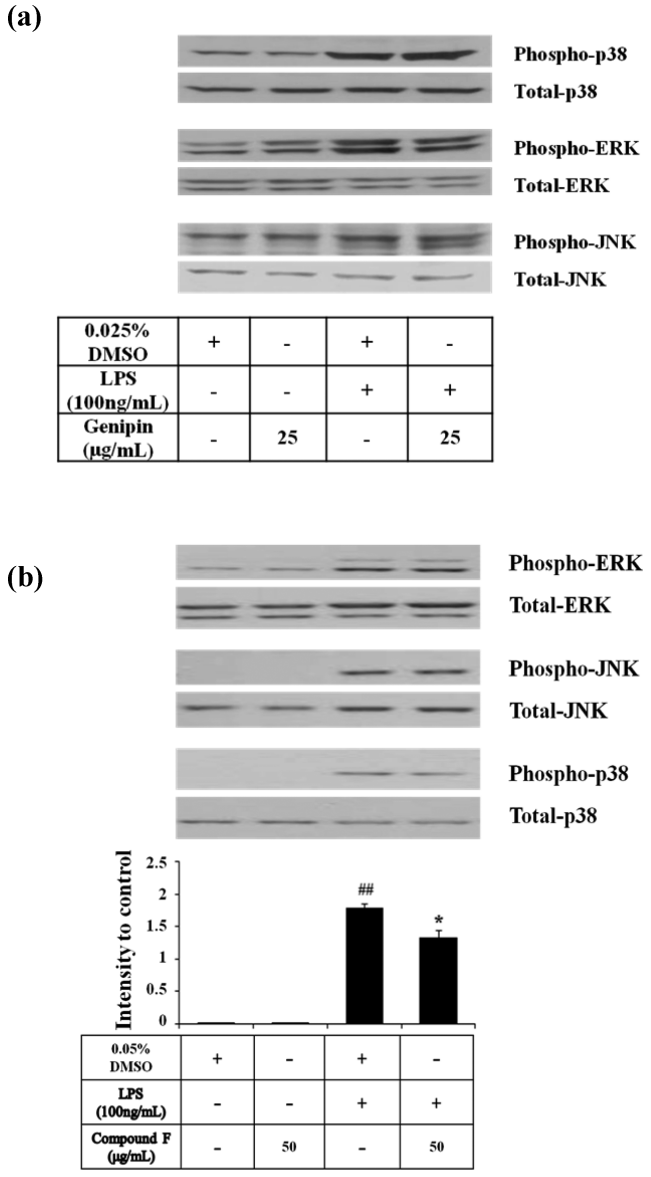

Figure 10. (a) Effect of genipin on p38 kinase, ERK, and JNK phosphorylation in LPS-stimulated BV-2 cells. BV-2 cells were pretreated with 25 μg/mL genipin for 2 h prior to the induction of LPS (100 ng/mL) for another 30 min. Cells were lysed for Western blotting. The figures are representative of three independent experiments. (b) Effect of compound F on p38 kinase, JNK, and ERK phosphorylation in LPS-stimulated BV-2 cells. BV-2 cells were pretreated with 50 μg/mL compound F for 2 h prior to the induction of LPS (100 ng/mL) for another 30 min. Cells were lysed for Western blotting using phosphorylated or total p38 kinase, JNK, and ERK antibodies. The figures are representative of three independent experiments. All data are presented as mean ± SD of three independent experiments. $^{\#\#}p < 0.01$, compared with DMSO group.$^{*}p < 0.05$, compared with DMSO + LPS group.

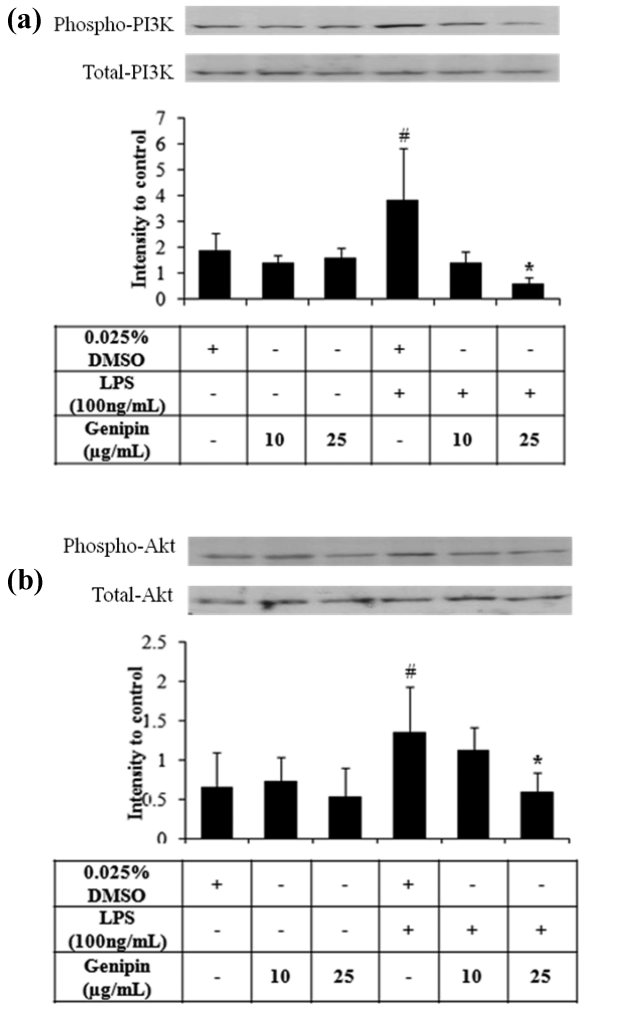

Figure 11. (a) Effect of genipin on PI3K phosphorylation in LPS-stimulated BV-2 cells. BV-2 cells were pretreated with genipin (10 and 25 μg/mL) for 2 h, followed by the stimulation of LPS (100 ng/mL) for another 3 h. Cells were lysed for Western blotting using phosphorylated or total PI3K antibodies. The figures are representative of three independent experiments. All data are presented as mean ± SD of three independent experiments. $^{\#}p < 0.05$, compared with DMSO group. $^{*}p < 0.05$, compared with DMSO + LPS group. (b) Effect of genipin on Akt phosphorylation in LPS-stimulated BV-2 cells. BV-2 cells were pretreated with genipin (10 and 25 μg/mL) for 2 h, followed by the stimulation of LPS (100 ng/mL) for another 3 h. Cells were lysed for Western blotting using phosphorylated or total Akt antibodies. The figures are representative of three independent experiments. All data are presented as mean ± SD of three independent experiments. $^{\#}p < 0.05$, compared with DMSO group. $^{*}p < 0.05$, compared with DMSO + LPS group.

stimulated phosphorylation of PI3K and Akt in a dose-dependent manner ($p < 0.05$). These results suggested that the suppressive effect of genipin on inducing TNF-α and iNOS is dependent on the PI3K/Akt signaling pathway, but not on the MAPK pathway. The PI3K/Akt pathway has been described to be involved in neurodegenerative diseases.[51−53] It could positively regulate pro-inflammatory gene expression in microglia and macrophages.[54−57] Several compounds had been demonstrated to inhibit PI3K/Akt phosphorylation. Cordycepin, isolated from *Cordyceps militaris*, inhibited the production of nitric oxide by down-regulation of iNOS gene expression through the suppression of Akt phosphorylation.[58] Acacetin, a flavonoid compound, inhibited the induction of NOS in LPS-stimulated RAW 264.7 cells by interfering with the activation of the PI3K/Akt pathway.[59] We further investigate its underlying mechanisms. The results suggested that genipin exerted its anti-inflammatory effects through the PI3K/Akt signaling pathway (Figure 11). Therefore, the PI3K/Akt pathway is a common target for the therapies of many inflammatory associated diseases.[60]

dx.doi.org/10.1021/cn5001205 | ACS Chem. Neurosci. 2014, 5, 855−866

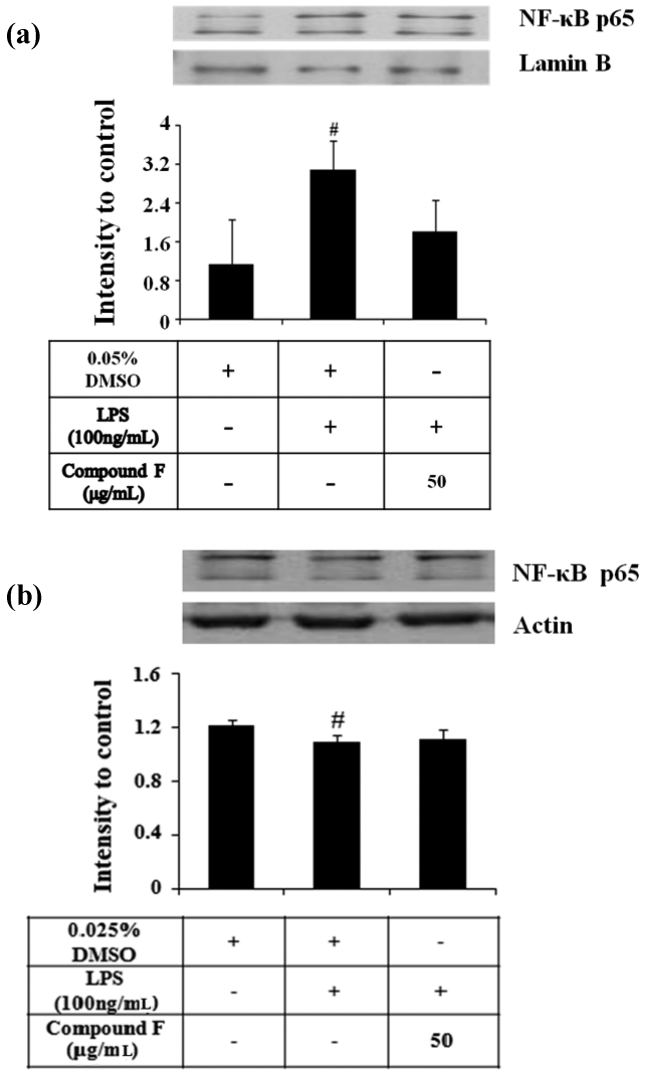

Figure 12. (a) Effect of compound F on NF-κB p65 in nuclear fraction in LPS-stimulated BV-2 cells. BV-2 cells were pretreated with compound F (50 μg/mL) for 2 h, followed by the stimulation of LPS (100 ng/mL) for another 30 min. Nuclear proteins were then extracted and immunoblotted with NF-κB p65 antibody. Lamin B was used to confirm the equal loading of samples. All data are presented as mean ± SD of three independent experiments. $^{\#}p < 0.05$, compared with DMSO group. (b) Effect of compound F on NF-κB p65 in cytosol fraction in LPS-stimulated BV-2 cells. BV-2 cells were pretreated with compound F (50 μg/mL) for 2 h, followed by the stimulation of LPS (100 ng/mL) for another 30 min. Cytoplasm proteins were then extracted and immunoblotted with NF-κB p65 antibody. Actin was used to confirm the equal loading of samples. All data are presented as mean ± SD of three independent experiments. $^{\#}p < 0.05$, compared with DMSO group.

In summary, genipin and compound F were isolated from DZ using a bioassay-guided fractionation scheme. Both genipin and compound F dose-dependently inhibited the production of NO and TNF-α in LPS-stimulated BV-2 cells. Moreover, they inhibited both mRNA levels and gene expression of iNOS. Genipin exerted its anti-inflammatory effect through suppressing PI3K/Akt activation, but not the MAPK signaling pathway. The suppressive effect of compound F was due to the inhibition of p38 kinase activation, whereas it did not exert any inhibitory effect on the translocation of NF-κB. Taken together, genipin and compound F can be considered as potential drug candidates for treating neurodegenerative diseases.

METHODS

Preparation of *Eucommia ulmoides* Oliver (DZ) Extract. Herb *Eucommia ulmoides* Oliver (DZ) was authenticated and obtained from PuraPharm International (H.K.) Ltd. The herbal powder was macerated in Milli-Q water (w/v: 1:8) for 2 h at room temperature and then boiled under reflux for another 2.5 h. After centrifugation at 10 000 rpm for 10 min, the supernatant was concentrated to dryness using a Rota-vap (Buchi, Germany).

Isolation of Anti-Inflammatory Compounds from DZ. We used a bioactivity-guided fractionation approach to isolate molecules with anti-inflammatory effects from herb DZ.[61] As NO is involved in neuroinflammation during pathological process of neurodegenerative diseases, we test the NO suppression effect of the extracts and compounds in LPS-induced BV-2 cells.

The extraction scheme of anti-inflammatory compound from DZ is summarized in Figure 1. First, the aqueous extract of DZ obtained under reflux was redissolved in methanol (MeOH) and then fractionated by partitioning with hexane (n-C_6H_{14}) (1:1). Then, the MeOH fraction was concentrated and redissolved in Milli-Q water and then sequentially partitioned with ethyl acetate (EtOAc) (1:1) and butanol (n-BuOH) (1:1) to yield four fractions including n-C_6H_{14}, EtOAc, BuOH and H_2O fractions. The EtOAc fraction (DZ-EA) with the strongest suppressive effect on LPS-stimulated NO production was further separated by silica gel column chromatography (pore size: 35−75 μm) using a series of solvent mixtures containing n-C_6H_{14}, EtOAc, and MeOH. A total of seven subfractions were obtained. The bioactive subfraction (DZ-EA-S1) was subjected to additional purification by C18 solid phase extraction (Sep-Pak Vac 6 cc/1 g, Waters) using acetonitrile (ACN) and water as the elution solutions. The bioactive fractions were combined and then further purified by reversed-phase high-performance liquid chromatography (HPLC) (Eclipse XDB-C18, 5 μm 4.6 × 250 mm, Agilent) at 1 mL/min flow with gradient elutions. The peaks were detected by using an Agilent Technologies 1200 Series fast scanning photodiode array detector with the detection wavelengths at 210, 254, and 280 nm. Finally, two single compounds with 95% purity were obtained.

Identification of Isolated Compounds. The molecular structures of compound C and F were elucidated using Bruker 500MH_Z and 600MH_Z PRX NMR spectrometers. Methanol-d was used as the solvent. Compounds were also indentified by GC-MS (GC, Agilent, 7890A; MS, Agilent, 5975C) using a HP-5MS column (30 m × 250 μm × 0.25 μm), and the GC condition used was similar to the ones used in our previous studies.[62,63] Briefly, one microliter of the sample was injected into the machine. Helium was used as the carrier gas in a flow of 1 mL/min. The oven temperature was started at 70 °C for 1 min, and then increased to 180 °C at a rate of 10 °C/min, and after 2 min holding increased to 300 °C at a rate of 20 °C/min and held for 5 min. The interface temperature was set at 250 °C. Mass spectra were analyzed in the range of 50−700 atom mass units (amu) for a run time of 25 min. The G1701EA chemstation (Agilent) was used to perform MS data analysis.

Cell Culture. The immortalized murine microglial BV-2 cell line was generously supplied by Prof. E Choi (Laboratory of Cell Death and Human Diseases, Korea University, Korea). It was cultured in Dulbecco's modified Eagle's minimum essential medium (DMEM) (Invitrogen) supplemented with 10% fetal bovine serum (FBS) (Sigma) and 1% antibiotics including penicillin and streptomycin at 37 °C in a humidified incubator containing 5% CO_2.

MTT Assay. BV-2 cells were seeded at 5 × 10^4 cells/mL in a 24-well plate. They were treated with different concentrations of herbal extracts and incubated for 48 h. MTT solution (Sigma-Aldrich) at the concentration of 0.5 mg/mL was added to the cells and incubated for 30 min at 37 °C. Isopropanol (IPP) was then added after removing the cell culture medium. After 10 min of incubation, the absorbance of each well was measured at 570 nm with a reference wavelength of 655 nm by using a microplate reader (model 680, Bio-Rad). The

dx.doi.org/10.1021/cn5001205 | ACS Chem. Neurosci. 2014, 5, 855−866

absorbance of each well was relative to the control well, and absorbances were expressed as percentages, that is, the percentage of the control well is 100%.[64]

Nitrite Measurement. BV-2 cells were seeded at a density of 1×10^5 cells/mL in a 24-well plate. Indicated concentrations of the compounds were added into the cells 2 h prior to the stimulation of 100 ng/mL LPS for 24 h. The culture supernatants were collected and transferred into a 96-well plate. An equal volume of Griess reagent (Sigma-Aldrich) was then added and incubated in the dark for 10 min. The absorbance of each well was measured at a wavelength of 570 nm. Nitrite levels were then determined by reference to the standard curve that was generated by the known concentrations of sodium nitrite.[65,66]

Reverse Transcription-Polymerase Chain Reaction (RT-PCR) and Quantitative RT-PCR. Total RNA was extracted by using TRIzol reagent (Invitrogen). The cDNA was synthesized from total RNA with oligo(dT) primer Superscript II Reverse Transcriptase (Invitrogen) as previously described.[67] The primer sequences were summarized as follows: GAPDH (T_m = 60 °C) forward, 5′-ACCACAGTCCATGCCATCAC-3′; reverse, 5′-TCCACCAC-CCTGTTGCTGTA-3′.[68] Mouse iNOS (T_m = 55 °C) forward, 5′-ACATCGACCCGTCCACAGTAT-3′; reverse, 5′-CAGAGGGG-TAGGCTTGTCTC-3′.[69] Mouse TNF-α (T_m = 56 °C) forward, 5′-ACGTGGAACTGGCAGAAGAG-3′; reverse, 5′-GTCTGGGCCAT-AGAACTGA-3′.[62] The PCR products were resolved by 1.5% agarose gel electrophoresis after staining with ethidium bromide. Visualization was performed under UV light with a Gel doc (Bio-Rad). The mRNA levels were also determined by QPCR (Roche 480II) as previously described.[62]

Enzyme-Linked Immunosorbent Assay (ELISA). BV-2 cells were seeded at the density of 1×10^5 cells/mL in a 24-well plate. They were pretreated with or without indicated concentrations of compounds for 2 h, followed by the 24 h incubation with 100 ng/mL LPS. The culture supernatants were collected for the determination of TNF-α level. ELISA kits (R&D Systems) were then used referring to the manufacturer's instructions.

Western Blot. BV-2 cells were seeded in a 12-well plate at a density of 2×10^5 cells/mL. They were treated with indicated concentrations of compounds for 2 h prior to being stimulated with (100 ng/mL) LPS for another 24 h (for iNOS) or 30 min (for MAPKs, NF-κB p65). Proteins were harvested by using SDS-lysis buffer. Protein concentrations were determined by using the bicinchoninic acid (BCA) protein assay kit (Pierce). The cytoplasmic proteins and nuclear proteins were extracted separately by Buffer A and Buffer C as described in our previous studies.[61,63,70] Protein concentrations were quantified using the Coomassie Plus Protein assay kit (Pierce). Equal amounts of total cellular protein were loaded per lane onto 10% SDS polyacrylamide gel electrophoresis (SDS-PAGE) and transferred onto the nitrocellulose membranes (Whatman Schleicher & Schuell, Germany). They were incubated with the indicated primary antibodies, including anti-iNOS (Sigma-Aldrich), anti-NF-κB p65, actin, lamin B (Santa Cruz Biotechnology), anti-phosphorylated and anti-total forms of p38 kinase, p42/p44 ERK, JNK, PI3K, and Akt (Cell Signaling Technology) overnight. After three washes, the membranes were incubated with the corresponding IgG HRP-conjugated secondary antibodies. Immunodetection was performed using ECL chemiluminesence kit (GE Healthcare) in the dark room.

Immunocytochemistry (ICC) Staining. BV-2 cells were seeded at 1×10^5 cells/mL onto 96-well plates. They were pretreated with 25 μg/mL genipin for 2 h before stimulation with (100 ng/mL) LPS. Culture media were removed after 30 min. Cells were then fixed in 4% paraformaldehyde (PFA) for 15 min at room temperature and washed twice with PBS before 0.1% Triton X-100 was added. After 5 min, cells were washed and blocked with 1% BSA in PBS for 5 min. Cells were washed again after a 3 h incubation with antibody against NF-κB p65 (1:1000) (Santa Cruz Biotechnology) in the dark at room temperature, followed by a 1 h incubation with a secondary antibody. Cells were then washed and incubated with DAPI solution for 5 min. Finally, cells were rinsed twice and analyzed by a Cellomics ArrayScan VTI (Thermo Scientific) instrument, which is distinguished for its automated and high capacity fluorescence imaging as well as quantitative analysis of live or fixed cells.

Statistical Analysis. Results were presented as mean ± SD, and the data were evaluated by one-way ANOVA followed by Tukey's or Dunnett test using SPSS (IBM). The p values less than 0.05 were considered statistically significant.

■ ASSOCIATED CONTENT

Supporting Information

Additional figures as described in the text. This material is available free of charge via the Internet at http://pubs.acs.org.

■ AUTHOR INFORMATION

Corresponding Authors

*E-mail: cindyy@hkucc.hku.hk. Phone: (+852)-25890535. Fax: (+852)-28175983.

*E-mail: drasylau@gmail.com.

Author Contributions

D.L., T.C.T.O., C.L.H.Y., and A.S.Y.L. designed the experiments; D.L. and C.L.H.Y. conducted the experiments; D.L., T.C.T.O., and C.L.H.Y. performed the data analysis. C.L.H.Y. and A.S.Y.L. conceived the project. D.L. wrote the manuscript.

Funding

This work was supported in part by grants from Prof. Francis S. K. Lau Research Fund and PuraPharm International (HK) Ltd. awarded to A.S.Y.L.

Notes

The authors declare no competing financial interest.

■ ACKNOWLEDGMENTS

We thank Prof. E. Choi from Laboratory of Cell Death and Human Diseases, Korea University for providing the BV-2 microglial cells. We also thank Gang Chen and Jian Zhou from PuraPharm International (Hong Kong) Limited for their technical support.

■ ABBREVIATIONS

DZ, *Eucommia ulmoides* Oliver; LPS, lipopolysaccharide; NO, nitric oxide; NMR, nuclear magnetic resonance; TNF-α, tumor necrosis factor-alpha; iNOS, inducible nitric oxide synthase; nNOS, neuronal NOS; eNOS, endothelial NOS; MAPK, mitogen-activated protein kinase; NF-κB, nuclear factor-κB; AD, Alzheimer's disease; PD, Parkinson's disease; ALS, amyotrophic lateral sclerosis; CNS, central nervous system; IL-1β, interleukin-1 beta; IL-6, interleukin-6; ROS, reactive oxygen species; NOS, nitric oxide synthase; MCAO, middle cerebral artery occlusion; JNK, C-Jun N-terminal kinase; ERK, extracellular signal-regulated kinase; HPLC, high performance liquid chromatography; TCM, traditional Chinese medicine; APP, amyloid precursor protein; NE, norepinephrine; EPI, epinephrine; LC, locus ceruleus; Aβ, amyloid-beta; FMLP, *N*-formyl-methionyl-leucyl-phenylalanine; MeOH, methanol; EtOAc, ethyl acetate; *n*-BuOH, butanol; ACN, acetonitrile; FBS, fetal bovine serum; IPP, isopropanol; RT-PCR, reverse transcription-polymerase chain reaction; ELISA, enzyme-linked immunosorbent assay; ICC, immunocytochemistry

■ REFERENCES

(1) Skaper, S. D., Giusti, P., and Facci, L. (2012) Microglia and mast cells: two tracks on the road to neuroinflammation. *FASEB J. 26*, 3103−3117.

(2) McGeer, P. L., Itagaki, S., Boyes, B. E., and McGeer, E. G. (1988) Reactive microglia are positive for HLA-DR in the substantia nigra of Parkinson's and Alzheimer's disease brains. *Neurology 38*, 1285−1291.
(3) Aloisi, F. (2001) Immune function of microglia. *Glia 36*, 165−179.
(4) Lucas, S. M., Rothwell, N. J., and Gibson, R. M. (2006) The role of inflammation in CNS injury and disease. *Br. J. Pharmacol. 147* (Suppl 1), S232−240.
(5) Zielasek, J., and Hartung, H. P. (1996) Molecular mechanisms of microglial activation. *Adv. Neuroimmunol. 6*, 191−122.
(6) Kaur, C., and Ling, E. A. (2009) Periventricular white matter damage in the hypoxic neonatal brain: role of microglial cells. *Prog. Neurobiol. 87*, 264−280.
(7) Andrew, P. J., and Mayer, B. (1999) Enzymatic function of nitric oxide synthases. *Cardiovasc. Res. 43*, 521−531.
(8) Pannu, R., and Singh, I. (2006) Pharmacological strategies for the regulation of inducible nitric oxide synthase: Neurodegenerative versus neuroprotective mechanisms. *Neurochem. Int. 49*, 170−182.
(9) Wang, P. H., and Zweier, J. L. (1996) Measurement of nitric oxide and peroxynitrite generation in the postischemic heart - Evidence for peroxynitrite-mediated reperfusion injury. *J. Biol. Chem. 271*, 29223−29230.
(10) Radi, R., Cassina, A., and Hodara, R. (2002) Nitric oxide and peroxynitrite interactions with mitochondria. *Biol. Chem. 383*, 401−409.
(11) Tweedie, D., Sambamurti, K., and Greig, N. H. (2007) TNF-alpha inhibition as a treatment strategy for neurodegenerative disorders: New drug candidates and targets. *Curr. Alzheimer Res. 4*, 378−385.
(12) Montgomery, S. L., and Bowers, W. J. (2012) Tumor Necrosis Factor-alpha and the Roles it Plays in Homeostatic and Degenerative Processes Within the Central Nervous System. *J. Neuroimmune Pharmacol. 7*, 42−59.
(13) McGeer, P. L., and McGeer, E. G. (2002) Local neuroinflammation and the progression of Alzheimer's disease. *J. NeuroVirol. 8*, 529−538.
(14) Yang, G. Y., Gong, C., Qin, Z., Ye, W., Mao, Y., and Bertz, A. L. (1998) Inhibition of TNFalpha attenuates infarct volume and ICAM-1 expression in ischemic mouse brain. *NeuroReport 9*, 2131−2134.
(15) Barone, F. C., and Feuerstein, G. Z. (1999) Inflammatory mediators and stroke: new opportunities for novel therapeutics. *J. Cereb. Blood Flow Metab. 19*, 819−834.
(16) Tian, D., Litvak, V., and Lev, S. (2000) Cerebral ischemia and seizures induce tyrosine phosphorylation of PYK2 in neurons and microglial cells. *J. Neurosci. 20*, 6478−6487.
(17) Walton, K. M., DiRocco, R., Bartlett, B. A., Koury, E., Marcy, V. R., Jarvis, B., Schaefer, E. M., and Bhat, R. V. (1998) Activation of p38(MAPK) in microglia after ischemia. *J. Neurochem. 70*, 1764−1767.
(18) Lee, M., McGeer, E., Kodela, R., Kashfi, K., and McGeer, P. L. (2013) NOSH-aspirin (NBS-1120), a novel nitric oxide and hydrogen sulfide releasing hybrid, attenuates neuroinflammation induced by microglial and astrocytic activation: A new candidate for treatment of neurodegenerative disorders. *Glia 61*, 1724−1734.
(19) Legos, J. J., Erhardt, J. A., White, R. F., Lenhard, S. C., Chandra, S., Parsons, A. A., Tuma, R. F., and Barone, F. C. (2001) SB 239063, a novel p38 inhibitor, attenuates early neuronal injury following ischemia. *Brain Res. 892*, 70−77.
(20) Barone, F. C., Irving, E. A., Ray, A. M., Lee, J. C., Kassis, S., Kumar, S., Badger, A. M., White, R. F., McVey, M. J., Legos, J. J., Erhardt, J. A., Nelson, A. H., Ohlstein, E. H., Hunter, A. J., Ward, K., Smith, B. R., Adams, J. L., and Parsons, A. A. (2001) SB 239063, a second-generation p38 mitogen-activated protein kinase inhibitor, reduces brain injury and neurological deficits in cerebral focal ischemia. *J. Pharmacol. Exp. Ther. 296*, 312−321.
(21) Schaeffer, V., Arbabi, S., Garcia, I. A., Knoll, M. L., Cuschieri, J., Bulger, E. M., and Maier, R. V. (2011) Role of the mTOR Pathway in LPS-Activated Monocytes: Influence of Hypertonic Saline. *J. Surg. Res. 171*, 769−776.
(22) Pacher, P., Beckman, J. S., and Liaudet, L. (2007) Nitric oxide and peroxynitrite in health and disease. *Physiol. Rev. 87*, 315−424.
(23) Wang, Q., Tang, X. N., and Yenari, M. A. (2007) The inflammatory response in stroke. *J. Neuroimmunol. 184*, 53−68.
(24) Buss, H., Schmitz, L., Dorrie, A., Resch, K., and Kracht, M. (2002) Characterisation of protein kinases targeting p65 NF-KB phosphorylation and transactivation. *Naunyn-Schmiedeberg's Arch. Pharmacol. 365*, R56−R56.
(25) Stone, J., Carson, A., Duncan, R., Roberts, R., Warlow, C., Hibberd, C., Coleman, R., Cull, R., Murray, G., Pelosi, A., Cavanagh, J., Matthews, K., Goldbeck, R., Smyth, R., Walker, J., and Sharpe, M. (2010) Who is referred to neurology clinics? The diagnoses made in 3781 new patients. *Clin. Neurol. Neurosurg. 112*, 747−751.
(26) Lang, C., Liu, Z., Taylor, H. W., and Baker, D. G. (2005) Effect of *Eucommia ulmoides* on systolic blood pressure in the spontaneous hypertensive rat. *Am. J. Chin. Med. 33*, 215−230.
(27) Freis, E. D., Ragan, D., Pillsbury, H., 3rd, and Mathews, M. (1972) Alteration of the course of hypertension in the spontaneously hypertensive rat. *Circ. Res. 31*, 1−7.
(28) Liu, E., Han, L., Wang, J., He, W., Shang, H., Gao, X., and Wang, T. (2012) *Eucommia ulmoides* bark protects against renal injury in cadmium-challenged rats. *J. Med. Food 15*, 307−314.
(29) Park, S. A., Choi, M. S., Jung, U. J., Kim, M. J., Kim, D. J., Park, H. M., Park, Y. B., and Lee, M. K. (2006) *Eucommia ulmoides* Oliver leaf extract increases endogenous antioxidant activity in type 2 diabetic mice. *J. Med. Food 9*, 474−479.
(30) Scatena, R., Martorana, G. E., Bottoni, P., Botta, G., Pastore, P., and Giardina, B. (2007) An update on pharmacological approaches to neurodegenerative diseases. *Expert Opin. Invest. Drugs 16*, 59−72.
(31) Lleo, A., Greenberg, S. M., and Growdon, J. H. (2006) Current pharmacotherapy for Alzheimer's disease. *Annu. Rev. Med. 57*, 513−533.
(32) Sarker, S. D., Latif, Z., and Gray, A. I. (2006) *Natural Products Isolation*, Human Press Inc., Clifton, NJ.
(33) Lelono, R. A., Tachibana, S., and Itoh, K. (2009) Isolation of antifungal compounds from *Gardenia jasminoides*. *Pak. J. Biol. Sci. 12*, 949−956.
(34) Mi, F. L. (2005) Synthesis and characterization of a novel chitosan-gelatin bioconjugate with fluorescence emission. *Biomacromolecules 6*, 975−987.
(35) Mailloux, R. J., Adjeitey, C. N., and Harper, M. E. (2010) Genipin-induced inhibition of uncoupling protein-2 sensitizes drug-resistant cancer cells to cytotoxic agents. *PLoS One 5*, e13289.
(36) Suzuki, Y., Kondo, K., Ikeda, Y., and Umemura, K. (2001) Antithrombotic effect of geniposide and genipin in the mouse thrombosis model. *Planta Med. 67*, 807−810.
(37) Tanaka, M., Yamazaki, M., and Chiba, K. (2009) Neuroprotective action of genipin on tunicamycin-induced cytotoxicity in neuro2a cells. *Biol. Pharm. Bull. 32*, 1220−1223.
(38) Goto, H., and Takikawa, H. (2010) Effect of genipin on cholestasis induced by estradiol-17beta-glucuronide and lithocholate-3-*O*-glucuornide in rats. *Hepatol. Res. 40*, 524−529.
(39) Lin, C. H., Chang, T. T., Sun, M. F., Chen, H. Y., Tsai, F. J., Chang, K. L., Fisher, M., and Chen, C. Y. (2011) Potent inhibitor design against H1N1 swine influenza: Structure-based and molecular dynamics analysis for M2 inhibitors from traditional Chinese medicine database. *J. Biomol. Struct. Dyn. 28*, 471−482.
(40) Koo, H. J., Song, Y. S., Kim, H. J., Lee, Y. H., Hong, S. M., Kim, S. J., Kim, B. C., Jin, C., Lim, C. J., and Park, E. H. (2004) Antiinflammatory effects of genipin, an active principle of gardenia. *Eur. J. Pharmacol. 495*, 201−208.
(41) Hwa, J. S., Mun, L., Kim, H. J., Seo, H. G., Lee, J. H., Kwak, J. H., Lee, D. U., and Chang, K. C. (2011) Genipin Selectively Inhibits TNF-alpha-activated VCAM-1 But Not ICAM-1 Expression by Upregulation of PPAR-gamma in Human Endothelial Cells. *Korean J. Physiol. Pharmacol. 15*, 157−162.
(42) Nam, K. N., Choi, Y. S., Jung, H. J., Park, G. H., Park, J. M., Moon, S. K., Cho, K. H., Kang, C., Kang, I., Oh, M. S., and Lee, E. H.

(2010) Genipin inhibits the inflammatory response of rat brain microglial cells. *Int. Immunopharmacol. 10*, 493−499.
(43) Zheng, L. T., Ryu, G. M., Kwon, B. M., Lee, W. H., and Suk, K. (2008) Anti-inflammatory effects of catechols in lipopolysaccharide-stimulated microglia cells: inhibition of microglial neurotoxicity. *Eur. J. Pharmacol. 588*, 106−113.
(44) Heneka, M. T., Nadrigny, F., Regen, T., Martinez-Hernandez, A., Dumitrescu-Ozimek, L., Terwel, D., Jardanhazi-Kurutz, D., Walter, J., Kirchhoff, F., Hanisch, U. K., and Kummer, M. P. (2010) Locus ceruleus controls Alzheimer's disease pathology by modulating microglial functions through norepinephrine. *Proc. Natl. Acad. Sci. U.S.A. 107*, 6058−6063.
(45) Chalermpalanupap, T., Kinkead, B., Hu, W. T., Kummer, M. P., Hammerschmidt, T., Heneka, M. T., Weinshenker, D., and Levey, A. I. (2013) Targeting norepinephrine in mild cognitive impairment and Alzheimer's disease. *Alzheimer's Res. Ther. 5*, 21.
(46) Kaneko, Y. S., Mori, K., Nakashima, A., Sawada, M., Nagatsu, I., and Ota, A. (2005) Peripheral injection of lipopolysaccharide enhances expression of inflammatory cytokines in murine locus coeruleus: Possible role of increased norepinephrine turnover. *J. Neurochem. 94*, 393−404.
(47) Tintinger, G. R., Theron, A. J., Anderson, R., and Ker, J. A. (2001) The anti-inflammatory interactions of epinephrine with human neutrophils in vitro are achieved by cyclic AMP-mediated accelerated resequestration of cytosolic calcium. *Biochem. Pharmacol. 61*, 1319−1328.
(48) Jan, B. U., Coyle, S. M., Oikawa, L. O., Lu, S. E., Calvano, S. E., Lehrer, P. M., and Lowry, S. F. (2009) Influence of acute epinephrine infusion on endotoxin-induced parameters of heart rate variability: A randomized controlled trial. *Ann. Surg. 249*, 750−756.
(49) Lipsanen, A., and Jolkkonen, J. (2011) Experimental approaches to study functional recovery following cerebral ischemia. *Cell. Mol. Life Sci. 68*, 3007−3017.
(50) Park, E. K., Rhee, H. I., Jung, H. S., Ju, S. M., Lee, Y. A., Lee, S. H., Hong, S. J., Yang, H. I., Yoo, M. C., and Kim, K. S. (2007) Antiinflammatory effects of a combined herbal preparation (RAH13) of *Phellodendron amurense* and *Coptis chinensis* in animal models of inflammation. *Phytother. Res. 21*, 746−750.
(51) Nakaso, K., Ito, S., and Nakashima, K. (2008) Caffeine activates the PI3K/Akt pathway and prevents apoptotic cell death in a Parkinson's disease model of SH-SY5Y cells. *Neurosci. Lett. 432*, 146−150.
(52) Jia, Y., Mo, S. J., Feng, Q. Q., Zhan, M. L., Ouyang, L. S., Chen, J. C., Ma, Y. X., Wu, J. J., and Lei, W. L. (2014) EPO-Dependent Activation of PI3K/Akt/FoxO3a Signalling Mediates Neuroprotection in In Vitro and In Vivo Models of Parkinson's Disease. *J. Mol. Neurosci. 53*, 117−124.
(53) Rickle, A., Bogdanovic, N., Volkman, I., Winblad, B., Ravid, R., and Cowburn, R. F. (2004) Akt activity in Alzheimer's disease and other neurodegenerative disorders. *NeuroReport 15*, 955−959.
(54) Kim, W. K., Hwang, S. Y., Oh, E. S., Piao, H. Z., Kim, K. W., and Han, I. O. (2004) TGF-beta1 represses activation and resultant death of microglia via inhibition of phosphatidylinositol 3-kinase activity. *J. Immunol. 172*, 7015−7023.
(55) Jhun, B. S., Jin, Q., Oh, Y. T., Kim, S. S., Kong, Y., Cho, Y. H., Ha, J., Baik, H. H., and Kang, I. (2004) 5-Aminoimidazole-4-carboxamide riboside suppresses lipopolysaccharide-induced TNF-alpha production through inhibition of phosphatidylinositol 3-kinase/Akt activation in RAW 264.7 murine macrophages. *Biochem. Biophys. Res. Commun. 318*, 372−380.
(56) Lee, J. Y., Jhun, B. S., Oh, Y. T., Lee, J. H., Choe, W., Baik, H. H., Ha, J., Yoon, K. S., Kim, S. S., and Kang, I. (2006) Activation of adenosine A3 receptor suppresses lipopolysaccharide-induced TNF-alpha production through inhibition of PI 3-kinase/Akt and NF-kappaB activation in murine BV2 microglial cells. *Neurosci. Lett. 396*, 1−6.
(57) Xing, B., Xin, T., Hunter, R. L., and Bing, G. (2008) Pioglitazone inhibition of lipopolysaccharide-induced nitric oxide synthase is associated with altered activity of p38 MAP kinase and PI3K/Akt. *J. Neuroinflammation 5*, 4.
(58) Kim, H. G., Shrestha, B., Lim, S. Y., Yoon, D. H., Chang, W. C., Shin, D. J., Han, S. K., Park, S. M., Park, J. H., Park, H. I., Sung, J. M., Jang, Y., Chung, N., Hwang, K. C., and Kim, T. W. (2006) Cordycepin inhibits lipopolysaccharide-induced inflammation by the suppression of NF-kappaB through Akt and p38 inhibition in RAW 264.7 macrophage cells. *Eur. J. Pharmacol. 545*, 192−199.
(59) Pan, M. H., Lai, C. S., Wang, Y. J., and Ho, C. T. (2006) Acacetin suppressed LPS-induced up-expression of iNOS and COX-2 in murine macrophages and TPA-induced tumor promotion in mice. *Biochem. Pharmacol. 72*, 1293−1303.
(60) Ghigo, A., Damilano, F., Braccini, L., and Hirsch, E. (2010) PI3K inhibition in inflammation: Toward tailored therapies for specific diseases. *BioEssays 32*, 185−196.
(61) Yang, C. L., Chik, S. C., Li, J. C., Cheung, B. K., and Lau, A. S. (2009) Identification of the bioactive constituent and its mechanisms of action in mediating the anti-inflammatory effects of black cohosh and related Cimicifuga species on human primary blood macrophages. *J. Med. Chem. 52*, 6707−6715.
(62) Or, T. C., Yang, C. L., Law, A. H., Li, J. C., and Lau, A. S. (2011) Isolation and identification of anti-inflammatory constituents from Ligusticum chuanxiong and their underlying mechanisms of action on microglia. *Neuropharmacology 60*, 823−831.
(63) Wang, L., Yang, C. L., Or, T. C., Chen, G., Zhou, J., Li, J. C., and Lau, A. S. (2011) Differential effects of Radix Paeoniae Rubra (Chishao) on cytokine and chemokine expression inducible by mycobacteria. *Chin. Med. 6*, 14.
(64) Marks, D. C., Belov, L., Davey, M. W., Davey, R. A., and Kidman, A. D. (1992) The MTT cell viability assay for cytotoxicity testing in multidrug-resistant human leukemic cells. *Leuk. Res. 16*, 1165−1173.
(65) Sreejayan, and Rao, M. N. (1997) Nitric oxide scavenging by curcuminoids. *J. Pharm. Pharmacol. 49*, 105−107.
(66) Or, T. C. T., Yang, C. L. H., Law, A. H. Y., Li, J. C. B., and Lau, A. S. Y. (2011) Isolation and identification of anti-inflammatory constituents from *Ligusticum chuanxiong* and their underlying mechanisms of action on microglia. *Neuropharmacology 60*, 823−831.
(67) Cheung, B. K. W., Yim, H. C. H., Lee, N. C. M., and Lau, A. S. Y. (2009) A novel anti-mycobacterial function of mitogen-activated protein kinase phosphatase-1. *BMC Immunol. 10*, 64.
(68) Kunert-Keil, C., Bisping, F., Kruger, J., and Brinkmeier, H. (2006) Tissue-specific expression of TRP channel genes in the mouse and its variation in three different mouse strains. *BMC Genomics 7*, 159.
(69) Niu, J., Azfer, A., Wang, K., Wang, X., and Kolattukudy, P. E. (2009) Cardiac-targeted expression of soluble fas attenuates doxorubicin-induced cardiotoxicity in mice. *J. Pharmacol. Exp. Ther. 328*, 740−748.
(70) Lee, D. C. W., Cheung, C. Y., Law, A. H. Y., Mok, C. K. P., Peiris, M., and Lau, A. S. Y. (2005) p38 mitogen-activated protein kinase-dependent hyperinduction of tumor necrosis factor alpha expression in response to avian influenza virus H5N1. *J. Virol. 79*, 10147−10154.